Original article

Formulation and characterization of propolis and tea tree oil nanoemulsion loaded with clindamycin hydrochloride for wound healing: *In-vitro* and *in-vivo* wound healing assessment

Menna M. Abdellatif [a],*, Yara E. Elakkad [b], Ahmed A. Elwakeel [c], Rasha M. Allam [d], Mohamed R. Mousa [e]

[a] Department of Industrial Pharmacy, College of Pharmaceutical Sciences and Drug Manufacturing, Misr University for Science and Technology, Giza, P.O. 12566, Egypt
[b] Department of Pharmaceutics, College of Pharmaceutical Sciences and Drug Manufacturing, Misr University for Science and Technology, Giza, P.O. 12566, Egypt
[c] Research Center, College of Pharmaceutical Sciences and Drug Manufacturing, Misr University for Science and Technology, Giza, P.O. 12566, Egypt
[d] Department of Pharmacology, National Research Center, Cairo, P.O. 12622, Egypt
[e] Department of Pathology, Faculty of Veterinary Medicine, Cairo University, Giza, P.O. 12211, Egypt

ARTICLE INFO

ABSTRACT

This study aimed to develop propolis and tea tree oil nanoemulsion loaded with clindamycin hydrochloride to heal wound effectively. Nanoemulsion formulae were prepared and characterized by droplet size analysis, zeta potential, viscosity, *ex-vivo* permeation, and skin deposition. The optimal formula was evaluated in terms of morphology, cytotoxicity, and *in-vitro* wound healing assay. Also, the efficacy of the optimal formula was evaluated by *in-vivo* wound healing and histopathological studies. The optimal formula (F3) was composed of 9% tea tree oil and 0.4% propolis extracts with mean droplet size 19.42 ± 1.7 nm, zeta potential value −24.5 ± 0.2 mV, and viscosity 69.4 ± 1.8 mP. Furthermore, the optimal formula showed the highest skin deposition value 550.00 ± 4.9 $\mu g/cm^2$ compared to other formulae. The TEM micrograph of the optimal formula showed that the nanoemulsion droplet has an almost spherical shape. Also, the optimal formula did not show noticeable toxicity to the human skin fibroblast cells. The *in-vitro* and *in-vivo* wound healing assay showed unexpected results that the un-loaded drug nanoemulsion formula had a comparable wound healing efficacy to the drug-loaded nanoemulsion formula. These results were confirmed with histopathological studies. Our results showed that the propolis and tea tree oil nanoemulsion, whether loaded or unloaded with an antibiotic, is an efficient local therapy for wound healing.

© 2021 The Author(s). Published by Elsevier B.V. on behalf of King Saud University. This is an open access article under the CC BY-NC-ND license (http://creativecommons.org/licenses/by-nc-nd/4.0/).

1. Introduction

Wound healing is a dynamic and complex skin repair process that responds to an injury or pathological conditions such as diabetes or vascular diseases. This process comprises overlapped but coordinated steps of inflammation, re-epithelialization, and remodeling (Oryan et al., 2018). It also involves immune and inflammatory cellular and biochemical events and requires the participation of several intracellular and extracellular metabolic regulation pathways. These activities aim to regain tissue integrity and restore local homeostasis (Dzobo et al., 2016). In several cases wound healing process is impaired as diabetes, infection, or metabolic deficiencies as Cushing Syndrome. Therefore, control of infection is a crucial step in the healing process. To prevent wound infection, synthetic drugs as antibiotics, chlorhexidine and silver have been used to kill bacteria and fungus (Oliveira et al., 2016). Also, natural products have been used due to their dual activity, namely antimicrobial and antioxidant activity; the latter may have an excellent role in the management of wound healing since the inflammation process leads to the accumulation of reactive oxygen species at the wound site, which may attack proteins and damage the cells, among the natural products to treat wounds, honey, propolis, Aloe vera, and Calendula officinalis (Pereira and Bártolo, 2016).

Propolis, also known as bee glue, is a resin made by bees collected from the buds, tree gum, or various botanical sources such as poplar, willow, birch, elm, alder, beech, conifer, and horsechestnut trees. Propolis has been used in traditional medicines for thousands of years due to its antibacterial and antifungal properties (Gavanji and Larki, 2017). In addition, studies pointed out further important activities of propolis as anti-inflammatory, antioxidant, and anti-tumor lesion restoration activities (Wagh, 2013; Gal et al., 2020). Finally, propolis reduces scar formation and healing time in skin wound healing, increases wound contraction and accelerates tissue repair (Olczyk et al., 2013). The biological activity of propolis is mainly due to substances such as flavonoids as galangin, hydroxycinnamic acids like caffeic acid, terpenes, phenolic, and esters (Berretta et al., 2012). In addition, propolis contains high amounts of vitamins as vitamin C, vitamin B, vitamin E, and provitamin A and minerals like copper, iron, calcium, zinc, cobalt, and potassium (Abdelrazeg et al., 2020).

Tea tree oil (TTO) is an essential oil extracted from the leaves of Melaleuca alternifolia. TTO is a mixture of volatile oil, terpenes, and lipoid substance. The main components of TTO include cycloolefins and enol compounds such as terpinen-4-ol, γ-terpinene, α-terpinene, 1,8-cineole, and α-terpineol (Battisti et al., 2021). TTO has a wide range of pharmacological actions, including antibacterial, antifungal, anti-inflammatory, antioxidant, anti-tumor, and immune regulation effects (Ramage et al., 2012). The antibacterial efficacy of TTO is well known, and it has been widely used in skin disinfection and skin or hair care products (Pazyar et al., 2013). For wound healing, Chin et al (Chin and Cordell, 2013) conducted a clinical study with patients suffering from wounds infected with Staphylococcus aureus. They concluded that TTO assists in the healing of abscessed wounds. However, TTO in pharmaceutical preparation is limited due to its irritancy, allergic reactions, volatility, instability upon exposure to light or oxygen, hydrophobicity, and formulation difficulties. Encapsulation of TTO at the nanoscale provides an efficient method to enhance the physical stability of the active compounds via., protection against volatilization and environmental reactivity (Flores et al., 2013).

Nanoemulsions (NEs), also known as miniemulsions, have tiny droplet sizes ranging from 20 to 500 nm. Unlike microemulsions, NEs have long-term thermodynamic stability; their structure depends on the process used to fabricate them and the steric stabilization obtained by adding non-ionic surfactants. Recently, NEs were extensively explored as novel carriers for successful topical delivery of essential drugs like curcumin, propofol, ibuprofen, and cyclosporine (Singh et al., 2017). TTO was successfully formulated as NEs in previous studies to enhance its stability (Wulansari et al., 2017). However, no study until now combines propolis and TTO in the same formulae.

Several studies pointed out the benefits of the combination of antibiotics with natural extracts to combat antibacterial resistance. Also, there is evidence to enhance conventional antibiotics by acting synergistically with natural compounds (Adwan et al., 2009; Cheesman et al., 2017). Clindamycin is an efficient antibiotic for healing severe skin and soft tissue infections, especially those caused by staphylococcus aureus (s. aureus) such as wound infection (Mikulášová et al., 2016). Therefore, the current study aimed to combine propolis and TTO with clindamycin hydrochloride as NEs formulae for wound healing. The prepared formulae were characterized for droplet size and zeta-potential. An *ex-vivo* permeation study was conducted to evaluate drug permeation and accumulation into the skin tissues. The optimal formula was selected and characterized in terms of morphology and cytotoxicity. *In-vitro* and *in-vivo* wound healing assay studies were conducted and confirmed with histopathological study to evaluate optimal formula wound healing efficiency.

2. Materials and methods

2.1. Materials

Clindamycin hydrochloride was kindly gifted by European Egyptian pharmaceutical industry company, Alexandria, Egypt, and lyophilized red propolis extract was purchased from VACSERA, Giza, EGYPT, tea tree oil was purchased from Sigma – Aldrich, Mumbai, India. All other reagents and solvents were of HPLC analytical grade obtained from Fisher Scientific Company, USA.

Dulbecco's Modified Eagle Medium, penicillin–streptomycin (100×), fetal bovine serum, and phosphate-buffered saline were purchased from Lonza Group Ltd., Basel, Switzerland. Sulforhodamine-B and trisaminomethane base were purchased from Sigma-Aldrich, Louis, MO, USA. Trichloroacetic acid was purchased from Merck, Darmstadt, Germany.

Sprague–Dawley rats without skin damage or diseases were obtained from Misr university for science and technology animal center (Giza, Egypt). The ethical committee approved all animal and cell lines studies of Misr university for science and technology (Approval No: PH 7).

2.2. Methods

2.2.1. Formulation of clindamycin hydrochloride loaded propolis and TTO NEs

Oil-in-water (O/W) NEs were formulated by dissolving tween-80 in distilled water containing the desired amount of clindamycin hydrochloride, as shown in Table 1. TTO and lyophilized propolis extract were added to the mixture with constant stirring at 500 rpm to form a coarse emulsion. Then, propylene glycol was added to the mixture. Then the system was probe sonicated (Sonics Vibra cell, BioBlock Scientific, France) for 3 min (30 sec on and 30 sec off). The system was ice jacketed to avoid any loss of essential oil.

2.2.2. Droplet size, distribution, and zeta potential

Droplet size, polydispersity index (PDI), and zeta potential (ZP) for NE formulae were measured by the dynamic light scattering (DLS) technique at 25 °C using Zetasizer (Malvern Instruments, Malvern, UK). The NE was properly five-folds diluted with purified water. Means and standard deviations were calculated for triplicates measurements.

2.2.3. Drug loading capacity

The ability of the NEs to load clindamycin hydrochloride was tested where the NEs formulae were centrifuged at 13000 rpm for 20 min to break up the emulsion (Rachmawati et al., 2015). The supernatant was withdrawn, and drug amount was analytically determined by the HPLC method, where a Luna C_{18} column was used with a mobile phase of (acetonitrile: buffer (pH 7.0) 60:40 (v/v %). The flow rate of the mobile phase was 1 mL/min, and UV detection at 210 nm was employed. The column was adjusted at 30 °C (Barakh Ali et al., 2019). The following equation calculated the loading capacity

$$Loading\ capacity\ \% = \frac{amount\ of\ drug\ encapsulated\ in\ NE}{amount\ of\ drug\ added\ to\ formula} \times 100$$

(1)

2.2.4. Viscosity

The viscosity of the NE samples was evaluated without further dilution using Brookfield DV III ultra V6.0 RV cone and plate rheometer (Brookfield Engineering Laboratories, Inc., Middleboro,

Table 1
Composition of NE Formulae, $n = 3$.

Composition	F1	F2	F3	F4	F5
Clindamycin %	1	1	1	–	–
TTO %	5	7	9	9	9
Propolis %	0.4	0.4	0.4	0.4	–
PG %	10	10	10	10	10
Tween 80%	20	20	20	20	20

TTO; tea tree oil, PG; propylene glycol.

MA) using spindle # CPE40 at 25 ± 0.5 °C. All the experiments were performed in triplicates. The spindle was set at 30 r.p.m and 60 s^{-1} as a shear rate, the measurements were conducted three times.

2.2.5. pH

The pH of NE formulae was tested using a calibrated potentiometer (Inolab pH 720, WTW, Germany) at ambient temperature. The measurements were conducted three times.

2.2.6. Ex-vivo skin permeation and deposition study

The skin for permeation experiments was excised from the dorsal area of healthy female Sprague–Dawley rats weighing 200–250 g. The hair was removed from the dorsal area without damaging the skin with a sufficient amount of an 8% sodium sulfide solution. After the rats were euthanized by cervical dislocation, the dorsal skin was surgically separated. Then, underlying fat and subcutaneous tissue were carefully removed. The full-thickness skin was washed with normal saline and stored at −20 °C (Lin et al., 2018). *Ex-vivo* permeation studies were carried out using modified Franz's diffusion cell with a diffusion area of 3.14 cm^2. The skin was fixed between the donor and receptor compartments. Accurately measured 1 mL of NE, equivalent to 10 mg of clindamycin hydrochloride, was placed in the donor cells. The receptor compartment filled with 30 mL of phosphate buffer saline solution (PBS) (pH 7.4) was maintained at 37 ± 1 °C under magnetic stirring at 100 rpm. Every hour 0.5 mL of permeation media was withdrawn for 6 h, and an equal volume of fresh media was added into the receiver cell. The samples were filtered through a 0.45 μm membrane and analyzed by using previously mentioned HPLC method. The results were reported as the mean of three runs. The amount of drug permeating through the skin was plotted versus time, and the permeability coefficient (cm/h) was determined according to the equation (Abdellatif et al., 2017):

$$Kp = Jss/C0 \qquad (2)$$

where Jss (steady stat flux) is the slope of the linear portion (μg/cm^2/h) and C0 is the initial drug concentration (μg/cm^2).

At the end of the study, the skin tissues were removed from the diffusion cell and washed in distilled water for 10 s to remove the adhering drug. The tissues were then cut into small pieces and sonicated in 5 mL methanol for 30 min using a bath sonicated to leach out the deposited drug. Finally, the samples were analyzed by the previously mentioned HPLC method.

2.2.7. Morphology

The NE formula with the highest skin deposition, ZP value, and lowest permeation profile was chosen for further assessment. The morphology of the optimal NE formula was analyzed using a transmission electron microscope (TEM) (JEM-1230, Joel, Tokyo, Japan). The sample was placed on the surface of a carbon-coated grid and negatively stained with a 1% aqueous solution of phosphotungstic acid and dried at room temperature. Afterward, the grid was observed using a TEM with an accelerating voltage of 120 kV.

2.2.8. Cytotoxicity assay

A human skin fibroblast cell line (HSF) was obtained from Nawah Scientific Inc. (Mokatam, Cairo, Egypt). Cells were maintained in Dulbecco's Modified Eagle Medium (DMEM) media supplemented with 100 mg/mL of streptomycin, 100 units/mL of penicillin, and 10% of heat-inactivated fetal bovine serum (FBS) in humidified, 5% (v/v) CO$_2$ atmosphere at 37 °C. Cell viability was assessed by sulforhodamine B (SRB) colorimetric assay. Aliquots of 100 μL cell suspension (5x10^3 cells) were seeded in 96-well plates and incubated in complete media for 24 h. Cells were treated with another aliquot of 100 μL media containing optimal NE formula (F3) at various concentrations (0.1,1,10,100,1000 ug/ml). After 72 h of drug exposure, cells were fixed by replacing media with 150 μL of 10% trichloroacetic acid (TCA) and incubated at 4 °C for 1 h. The TCA solution was removed, and the cells were washed five times with distilled water. Aliquots of 70 μL SRB solution (0.4% w/v) were added and incubated in a dark place at room temperature for 10 min. Plates were washed three times with 1% acetic acid and allowed to air-dry overnight. Then, 150 μL of trisaminomethane base solution (TRIS) (10 mM) was added to dissolve the protein-bound SRB stain; the absorbance was measured at 540 nm using a BMG LABTECH®- FLUOstar Omega microplate reader (Ortenberg, Germany) (Paknejadi et al., 2018).

2.2.9. In-vitro wound healing assay

HSF cells were seeded at density 5x10^3 well onto a coated 6-well plate for scratch wound assay and cultured overnight in 5% FBS - DMEM at 37 °C and 5% CO$_2$. The next day, horizontal scratches were introduced into the confluent monolayer; the plate was washed thoroughly with PBS. Control wells were replenished with the fresh medium, while drug wells were treated with fresh media containing different formulae. Images were taken using an inverted microscope at 0, 24,48,72, and 96 h, as shown in Fig. 1. The plate was incubated at 37 °C and 5% CO$_2$ in-between time points. The images were analyzed by MII Image view software version 3.7. For each image, the gap area was measured at certain time intervals and was compared to the initial gap area at time t = 0. Wound closure (expressed as a percentage) was calculated from the following equation (Main et al., 2020):

$$Wound\ closure\ (\%) = (Wt_0 - Wt_i)/Wt_0 \times 100 \qquad (3)$$

Wt$_0$ is the initial wound area at the outset of the experiment, and Wt$_i$ is the measured wound area at a given time interval.

2.2.10. In-vivo wound healing assay

Sprague–Dawley rats, 150–200 gm, were given 4×3 cm^2 dorsal full-thickness excisions under anesthesia with 50 mg/kg intraperitoneal pentobarbital (Mohamed et al., 2020). The procedures were approved by the Ethical Committee of Misr University for science and technology (reference number: PH 7) and followed the guidelines for the care and use of laboratory animals published by US NIH publication No. 85–23. The rats were divided into five groups, each of 6 as shown in Table 2, and the wounds were treated with 50 mg of topical formulae twice daily for 14 days. Care was taken not to traumatize the wound. Wound surface area was measured
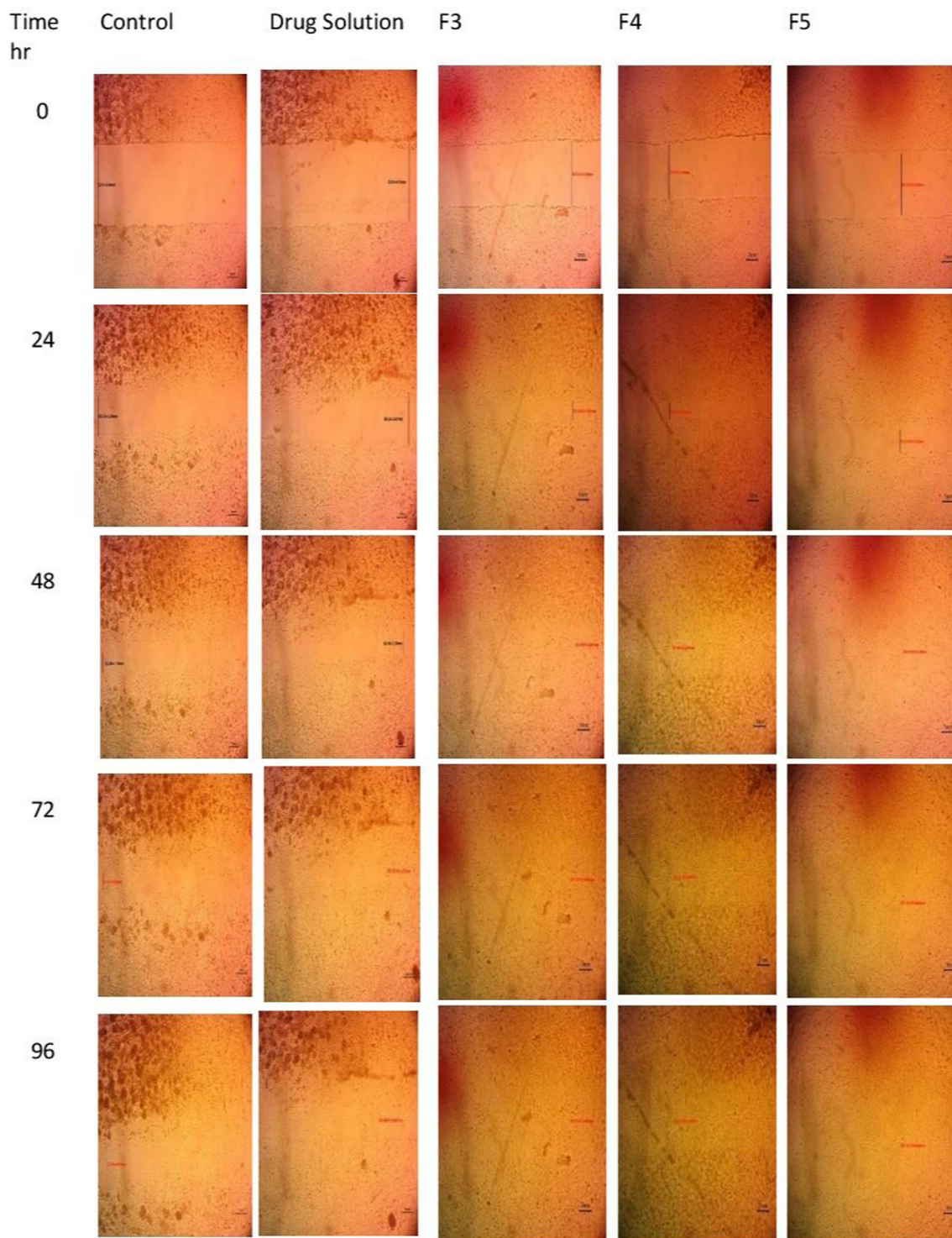
Fig. 1. The images of scratch wound assay of different formulae at different time intervals.

Table 2
In-vivo wound healing assay using different formulae.

Group name	Treatment
GP 1	F3
GP2	F4
GP 3	F5
GP 4	1% Clindamycin solution
GP 5	Distilled water

by radial planimetry every five days (Hasan et al., 2019). The rats were kept in individual wire-bottom cages in a room with a 12-h light/dark cycle and allowed to feed on rat chow and take water. Wound closure percent was calculated as mentioned before in section methods 2.2.9.

2.2.11. Histopathology study

Tissue samples from the skin wound were collected on day 5, where three rats were sacrificed from each group and on day 14

(at the end of the experiment). Skin tissues from both the wounded and comparable contralateral normal skin were dissected and washed with ice-cold saline, then fixed in 10% neutral-buffered formalin (10% neutral buffered formalin was composed of 4 gm of monobasic sodium phosphate, 6.5 gm of dibasic sodium phosphate, 100 mL of commercial formaldehyde (37–40%), and 900 mL distilled water, pH was adjusted to be 7.2 ± 0.5). The skin samples were routinely processed, stained with H&E and Masson's trichrome (MTC) stains, and examined under a light microscope. Histologic scoring was done by giving a score ranging from 0 to 4 for each of the following criteria: re-epithelization, granulation tissue formation, inflammation, and angiogenesis. For re-epithelialization (0 = lack of epithelial cover, 1 = Poor epidermal remodeling, 2 = Partial epidermal formation, 3 = Moderate epithelial proliferation, and 4 = Complete re-epithelization). For granulation tissue formation; (0 = young and inflamed granulation, 1 = less immature and inflammatory tissue, 2 = Moderate remodeling, 3 = Thick granulation layer, abundant collagen, and 4 = full organized healthy tissue). For the inflammatory degree (0 = 13–15 inflammatory cells per microscopic field, 1 = 10–13 inflammatory cells per microscopic field, 2 = 7–10 inflammatory cells per microscopic field, 3 = 4–7 inflammatory cells per microscopic field, and 4 = 1–4 inflammatory cells per microscopic field). For angiogenesis (0 = missing of angiogenesis with congestion, hemorrhage, and edema, 1 = 1–2 vessels per field with edema, hemorrhage, and congestion, 2 = 3–4 vessels per field, moderate edema, and congestion, 3 = 5–6 vessels per field with slight edema and congestion, 4 = >7 vessels per field vertically oriented on the epidermal layer) (Hosseini et al., 2011).

2.3. Statistical analysis of data

To investigate the significant difference between the results of the studied formulae, the one-way analysis of variance (ANOVA) test was used. The level of significance was set at 0.05, and ($p < 0.05$) was statistically significant.

3. Results and discussion

3.1. Droplet size analysis, distribution, and zeta potential

Based upon previous studies that discussed the formulation of TTO NEs, the percentage of TTO was varied from 5 to 9%, with a surfactant concentration ranged from 15 to 30% (Najafi-Taher et al., 2018; Sinha et al., 2016; Wulansari et al., 2017). Our study aimed to obtain the optimal concentration of TTO in the nanoemulsion formulation rather than studying the impact of surfactant and co-surfactant ratios upon formulations aspects which was handled in the previous studies; therefore, we used a varied concentration of TTO with a constant concentration of surfactant and cosurfactant.

The results of NEs characterization showed that the droplet size of all NE formulae was in the nano range, as shown in Table 3. The droplet size increased with the increased concentration of TTO in the formulae. Thus, increasing the internal dispersed phase, resulting in an increasingly large droplet size (Wulansari et al., 2017). The mean droplet size of the main NE formulae (F1-F3) ranged from 11.71 ± 0.8 nm to 19.42 ± 1.7 nm. These results agree with the size range reported by Sinha et al. (2016). Upon reviewing the data obtained from control formulae (F3 &F4), we found that the absence of the drug did not significantly affect mean droplet size (p > 0.05), where the mean droplet size of (F3) was 19.42 ± 1. 7 nm and the mean droplet size of (F4) was 20.64 ± 1.9 nm; however, the absence of 0.4% propolis led to a significant reduction in mean droplet size from 19.42 ± 1.7 nm (F3) to 10.90 ± 0.6 nm (F5). These results agree with Ghavidel et al. (2021), who found that by increasing the amounts of propolis extract in NEs formulae, the nanodroplet size was increased because of agglomeration of the formed propolis nanodroplets in NEs. The PDI value lower than 0.3 indicated the uniformity of the droplet size distribution.

The zeta potential is an essential parameter in determining a dispersion system's stability and the possibility of flocculation or aggregation in the emulsion and suspension system (Sari et al., 2015). It was previously reported that negative ZP values higher than 20 mV were sufficient to prevent droplet coalescence in the NEs formulae (Oh et al., 2011). In our study, the ZP values ranged from – 7.91 to – 25.1 mV. Only formulae composed of 9% TTO showed a ZP value above 20 mV, indicating that TTO was the predominant factor for imparting negative surface charge on the NE droplet. Also, the surfactant (tween 80) used here was a non-ionic surfactant (Najafi-Taher et al., 2018). Li et al. (2016) suggested that the low surface charge of TTO NE would favor the contact of formulae with microbial cells. Although the low value of zeta potential, the NE formulations remained transparent after storing for 60 days at refrigerator temperature (2–8 °C), confirming the stability of the nanoemulsion system. There was no significant difference regarding zeta values between (F3) and the control formulae (F4& F5), suggesting that the drug and propolis had no significant impact on zeta potential value.

3.2. Drug loading capacity

The water-soluble drug (clindamycin hydrochloride) was successfully loaded into propolis and TTO NE, where the loading capacity ranged from 91.20 to 89.02%, as shown in Table 3.

3.3. Viscosity

The viscosity of the NE formulations showed a low viscosity value, as shown in Table 3. In general, NE formulations are usually characterized by low viscosity (Akhtar et al., 2016). Increasing the TTO concentration from 5 to 9% did not significantly affect the viscosity of the NE formulations indicating that the concentration of surfactants had a significant effect on viscosity.

Table 3
Characteristics of NE Formulae, n = 3.

Formulation Code	Characteristics					
	Droplet size nm	PDI	ZP mV	Viscosity mP	Loading capacity %	pH
F1	11.71 ± 0.8	0.17	−7.91 ± 0.72	68.8 ± 2.3	91.20 ± 1.98	7.2 ± 0.02
F2	15.90 ± 1.1	0.22	−14.5 ± 0.58	60.2 ± 1.3	89.02 ± 1.47	7.1 ± 0.05
F3	19.42 ± 1.7	0.24	−24.5 ± 0.2	69.4 ± 1.8	89.53 ± 1.86	7.2 ± 0.07
F4	20.64 ± 1.9	0.24	−25.1 ± 1.1	66.7 ± 2.1	–	7.1 ± 0.05
F5	10.90 ± 0.6	0.18	−23.2 ± 0.9	68.9 ± 0.5	–	7.0 ± 0.02

PDI; Polydispersity index, ZP; zeta potential.

3.4. pH

The observed pH value for all formulae was 7.1 ± 0.08, which is considered suitable for dermal application (Salim et al., 2016).

3.5. Ex-vivo skin permeation study

Fig. 2 demonstrates the skin permeation of the drug from various NEs. The flux values decreased from 477.18 ± 0.57 µg/cm^2/h (F1) to 395.38 ± 0.63 µg/cm^2/h (F2) followed by a further decrease to 226.97 ± 0.76 µg/cm^2/h (F3) as shown in Table 4, suggesting a negative effect of increasing oil concentration on drug permeation through skin layers, this may be due to the increased droplet size upon increasing oil concentration. In general, there was a reduction in permeation parameters upon the increasing concentration of TTO in NEs formulae, where the total amount permeated after 6 h (Q_6) was significantly decreased (p < 0.05) from 2325.28 ± 0.99 µg/cm^2 (F1) to 1895.42 ± 0.88 µg/cm^2 (F2) followed by a further decrease to 1246.14 ± 0.82 µg/cm^2 (F3). The permeability coefficient (Kp) was also decreased from 0.047 ± 0.030 cm/h (F1) to 0.039 ± 0.039 cm/h (F2), followed by a further decrease to 0.022 ± 0.055 cm/h (F3). The viscosity of topical formulae might also affect the drug permeation across the skin as the low viscosity formulae make the active substance move more easily than high viscosity because of the inverse relation between viscosity and drug release property (Tas et al., 2007). In our present study, the NEs formulae were characterized by low viscosity values. As mentioned before, there was no significant effect of increasing TTO concentration from 5 to 9% on the viscosity of the NE formulae, indicating that the predominant effect on drug permeation across the skin was droplet size. Since the NE formula is designed to treat wounds, more skin retention is required rather than permeation (Thomas et al., 2017). Therefore, skin deposition of the clindamycin hydrochloride in the three formulations was investigated and found in 177.78–550.00 µg/cm^2. Since the highest skin deposition and the lowest permeation profile were obtained by formula (F3), therefore it was selected for further studies.

3.6. Morphology

The TEM micrograph of optimal formula (F3) showed that the NE droplet appeared dark with an almost spherical shape, as shown in Fig. 3. In addition, the droplet size of the (F3) determined by Zetasizer was in good agreement with TEM observations.

3.7. Cytotoxicity assay

Before the *in-vivo* assay of the formulations, an appropriate in-vitro cytotoxicity study was performed to evaluate their safety. Among present accessible techniques for *in-vitro* cytotoxicity
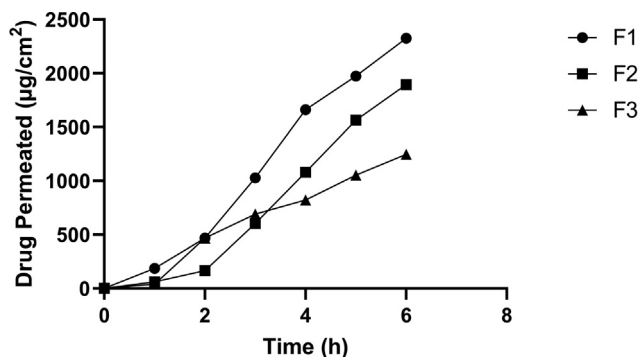

Fig. 2. *Ex-vivo* permeation profile of different formulae.

screening tests, SRB colorimetric assay is the preferred method, especially for screening activity of natural compounds. It provides better linearity and reproducibility, less sensitivity to environmental variations, and independence to intermediate metabolism (Papadimitriou et al., 2019). The formulation was developed for topical application on the skin, and the cytotoxicity testing using cultured human skin cells is a valuable model for skin damage assessment. The (F3) formula did not show remarkable toxicity against HSF cells even at the utilized high concentrations (100 and 1000 ug/mL), maintaining cell viability $\geq$ 65% compared to untreated HSF cells and possessing IC50 value > 1000 µg/mL as shown in Fig. 4. These results were consistent with the previous study of Homeyer et al. (2015), who demonstrated the concentration-dependent cytotoxicity of TTO on the skin fibroblast cells. Furthermore, these results were more advantageous to the study performed by Shehata et al. (2020). They found that the cytotoxicity of propolis alone against HSF cells with IC50 values between 100 and 1000 ug/mL.

3.8. In-vitro wound healing assay

The safety behavior of the F3 formula shown in the cytotoxicity study inspires the evaluation of its *in-vitro* wound healing activity. Therefore, we aimed to investigate the effect of NE components on wound healing activity, and the optimal formula (F3) was used as a reference to formulate other formulae. Therefore, F4, F5, and 1% clindamycin solution were prepared as mentioned before in the methods section. The maximum wound closure percent was detected by F3 and F4 (60.0639 ± 0.335%,61.33 ± 0.150%) respectively, and there was no significant difference between both formulae at different time intervals (p > 0.05) as shown in Fig. 5. Accordingly, these results ruled out the effect of clindamycin hydrochloride in the process of *in-vitro* wound healing and showed the superiority of the NE base components of these formulae (F3 and F4). These results were confirmed by *in-vitro* testing the efficacy of 1% drug solution on the wound healing process. There was no significant difference between percent closure observed at any time interval by drug solution and the control (p > 0.05). However, the F5 formula (NE formula without propolis and drug) showed no significant difference in wound healing activity comparing with the control results, indicating that the *in-vitro* wound healing efficacy of propolis and TTO NE was due to the presence of propolis. These results could be explained by understanding the ability of propolis in promoting the skin wound healing activity through the stimulation of epithelial regeneration, modulation of extracellular matrix deposition, and facilitating the formation of granulation tissue (Pessolato et al., 2011; Gheib et al., 2020). The lack of the in-vitro wound healing activity of TTO may be explained as TTO exerts its wound healing efficacy mainly through its antimicrobial role.

3.9. In-vivo wound healing assay

The results obtained from *in to vivo* wound healing were somewhat like those obtained from *in to vitro* wound healing study where there was no significant difference between GP (1) and GP (2) (p > 0.05) at all time intervals, as shown as in Fig. 6. The rate of wound closure obtained by both groups (1&2) was much faster than the other groups. On the other hand, there was a significant difference between GP (3) and the control GP (5) (p < 0.05) and the drug solution GP (4) and the control GP (5) (p < 0.05), this may be due to the presence of Staphylococcus aureus on rat skin which usually considered as skin transient flora. As infected skin tends to heal slowly, the presence of antimicrobial agents either as TTO or drug solution in the treatment of groups (3&4) led to a significant increase in wound closure percentage compared to

Table 4
Permeation parameters of different formulae, $n = 3$.

Formulae	Jss ($\mu g/cm^2/h$)	K_p (cm/h)	Q_6 ($\mu g/cm^2$)	Skin deposition ($\mu g/cm^2$)
F1	477.18 ± 0.57	0.047 ± 0.030	2325.28 ± 0.99	177.78 ± 4.3
F2	395.38 ± 0.63	0.039 ± 0.084	1895.42 ± 0.88	236.75 ± 3.7
F3	226.97 ± 0.76	0.022 ± 0.055	1246.14 ± 0.82	550.00 ± 4.9

Jss; steady-state flux, K_P; permeability coefficient; Q_6; Total amount of drug permeated per unit area after 6 h.
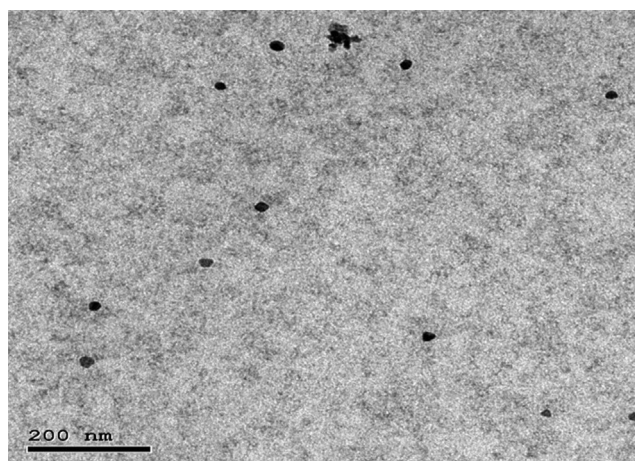
Fig. 3. Transmission electron microscope (TEM) image of the optimal NE formula (F3).

Fig. 6. Percentage of wound closure of different formulae (In-vivo wound healing assay).
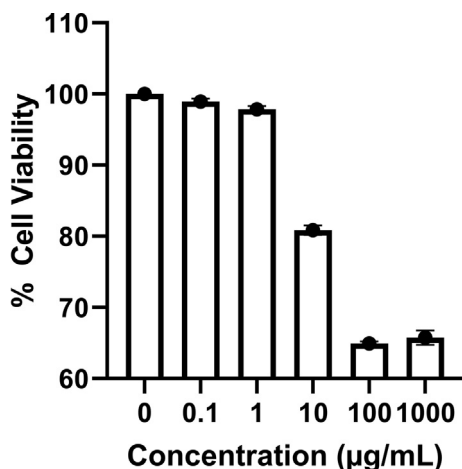
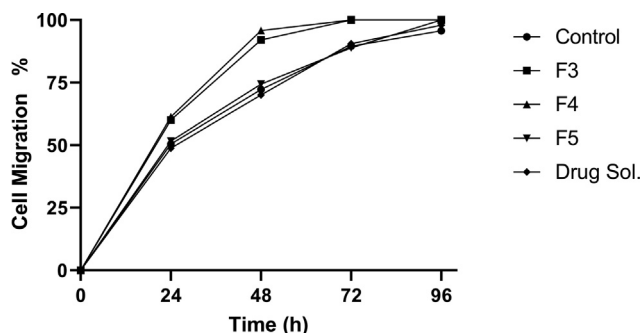**Fig. 4.** The percentage of viability was determined by SRB assay after treating human skin fibroblast (HSF) cells with F3.

Fig. 5. *In-vitro* wound healing activity of different formulae presented as a percentage of wound closure at various time intervals.
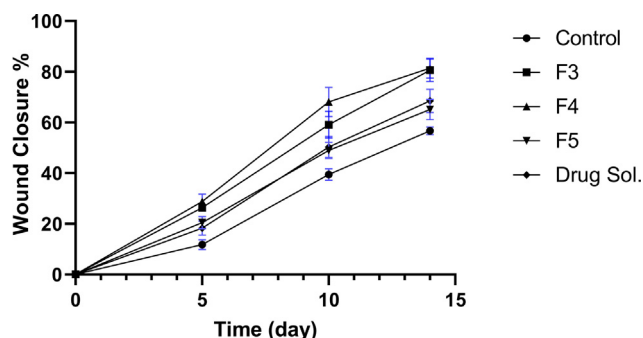
the control group at all time intervals. There was no significant difference between GP (3) and GP (4) at all time intervals revealing that TTO exerted comparable antimicrobial efficacy to clindamycin hydrochloride against skin transient flora. These results agree with Muta et al. (2020), who found that TTO lipid-based nanoformulation (5% TTO) exhibited bitter antibacterial activity against *S. epidermidis* than kanamycin.

3.10. Histopathology study

The histopathological alterations and lesion scores were assessed in all groups on day 5 postoperative, as shown in Fig. 7. On the fifth day after the injury, the animals of treated groups showed differences in healing times and microscopic inflammation compared with the animals of the control group. GP (1) and (2) showed inflammatory reactions similar to that noticed in the control group. However, the areas of hemorrhages and necrosis were limited to few examined sections. Additionally, signs of re-epithelization were observed at the wound edges. GP (3) showed similar histopathological alterations to GP (4). However, less necrosis was scored in some instances accompanied by hyperplastic newly formed epidermal growth was starting at the wound edge. GP (4) showed moderate inflamed granulation tissue admixed with newly formed blood vessels filling the wound cavity with extensive edema leading to dispersion of the formed inflamed tissue. The superficial surface of the wound gap was filled with abundant necrotic tissue covered by serocellular crust rich in neutrophils infiltration. Control GP (5) showed intense inflammatory granulation tissue occupying the wound gap characterized by extensive neutrophilic infiltration admixed with numerous reactive fibroblasts with newly formed congested blood capillaries and edematous exudates. The wound surface is covered by serocellular crust with transmigration of neutrophils in the formed crust and abundant underneath necrosis and hemorrhage in most examined sections. Histopathological lesion score (Fig. 8) showed a significant improvement in epidermal remodeling and granulation tissue formation in GP (1) and GP (2) in comparison with GP (5). The inflammation was numerically improved in all treated groups compared to the wounded untreated group (GP (5)). Although all treated groups showed a numerical enhancement in the angiogen-
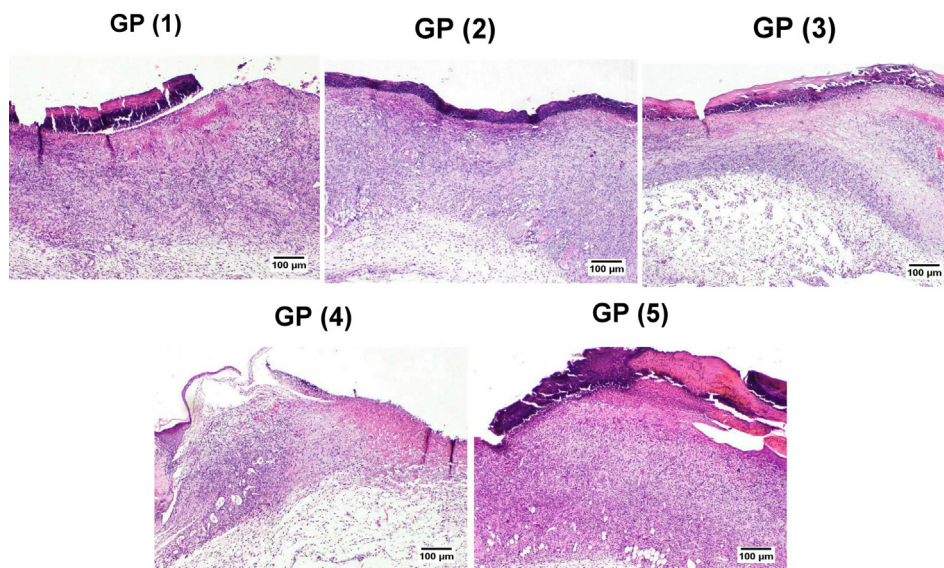
Fig. 7. Histopathological examination of tissue samples from the skin wound collected on day 5 from the different groups (H&E).
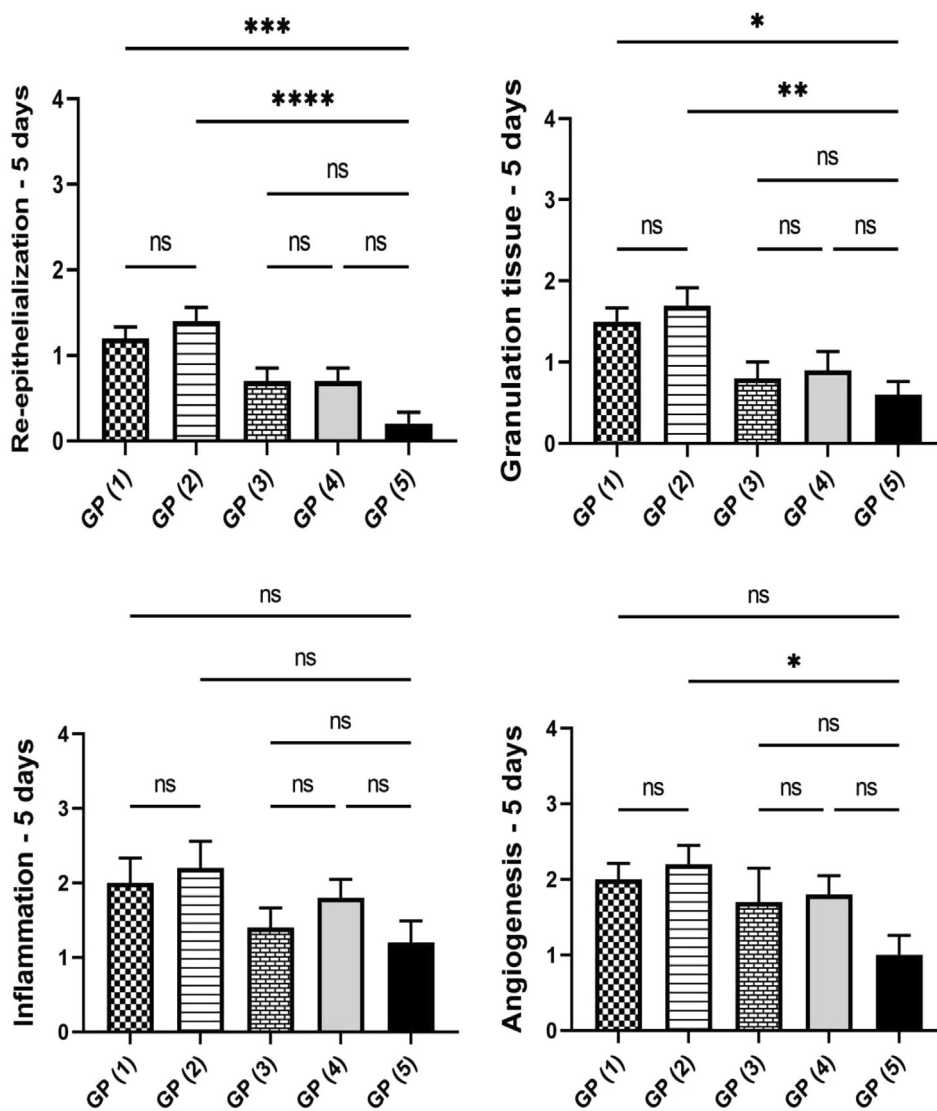

Fig. 8. Charts present histological scores among different groups on day 5. Data Expressed as means ± standard error. A significant difference is considered at p < 0.05.

Fig. 9. Histopathological examination of tissue samples from the skin wound collected on day 14 from the different groups (H&E).

Fig. 10. Charts present histological scores among different groups on day 14. Data Expressed as means ± standard error. A significant difference is considered at p < 0.05.
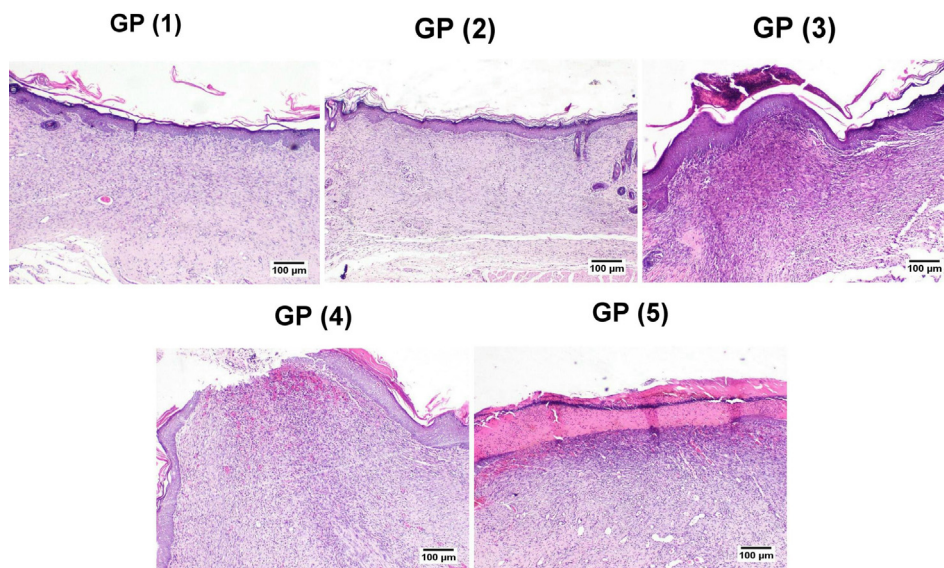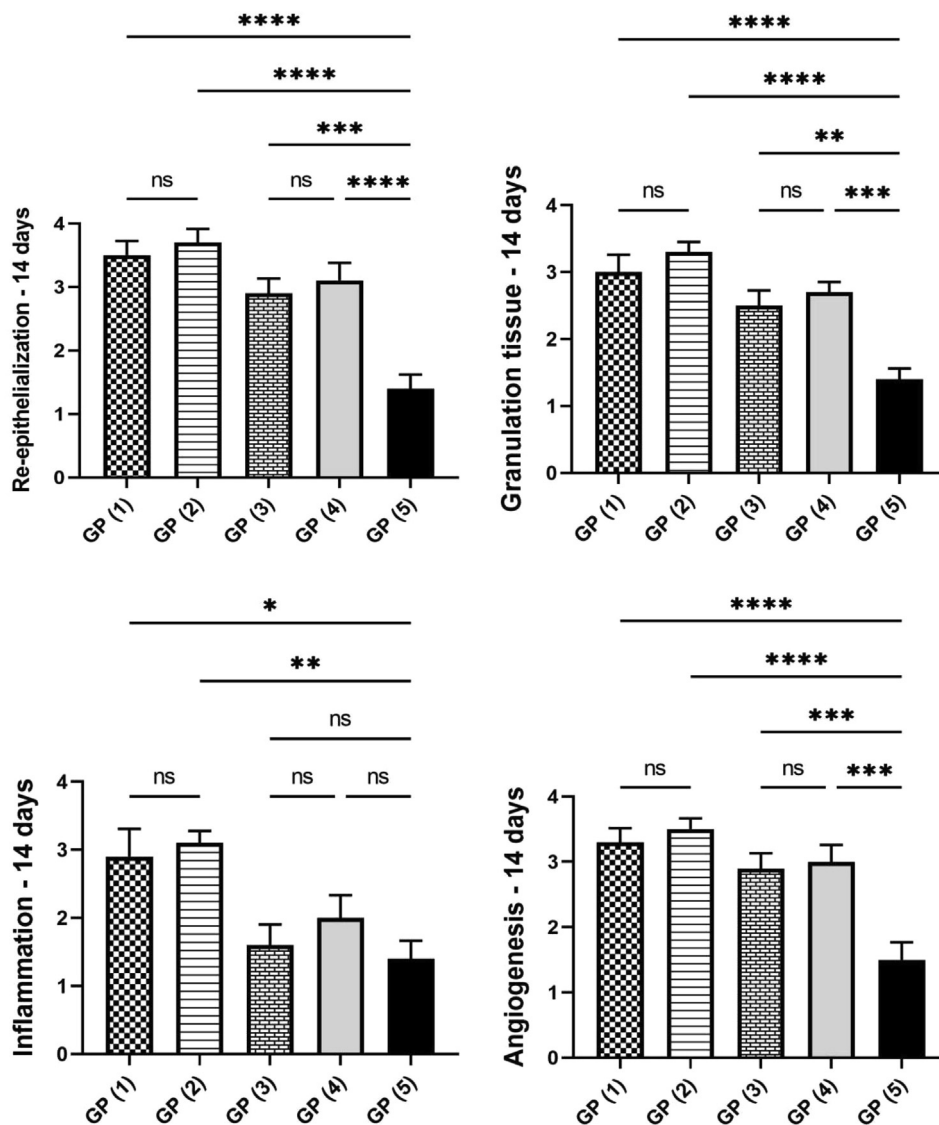
esis formation compared with GP (5), the only statistically significant difference was scored by GP (2).

On day 14 (Fig. 9), GP (1) and (2) showed the best wound healing among different experimental groups. A well-formed organized tissue rich in collagen bundles was noticed filling the wound cavity with few to the absence of the inflammatory reaction. A thick epidermal layer covered the wound surface with newly formed blood capillaries below and evidence of keratinization. GP (3) showed the formation of granulation tissue with less inflammation than GP (5), and the re-epithelization appeared thick epidermal layer covering the wound surface in some examined sections. Meanwhile, others exhibited thin epidermal growth that showed incomplete covering of the wound area. GP (4) showed well-organized tissue occupying the wound space with better signs of re-epithelization, and marked

keratinization occurred in most examined sections. Few sections showed an advanced grade of wound healing except for the wound center, which revealed no epithelial covering with marked superficial inflammation and severely congested capillaries. GP (5) showed less organized granulation tissue with persistent abundant inflammatory cells infiltration, which was heavily presented in the superficial wound surface. Re-epithelization was noticed at the wound edges, with a thick eosinophilic crust covering almost the wound gap. Referring to the re-epithelization and angiogenesis scores (Fig. 10), a significant increase was recorded in all treated groups compared to GP (5). The grade of the formed granulation tissue was significantly lower in GP (5) compared to the other groups. Similarly, the inflammation appeared more intense in GP (5) compared to the other experimental groups.
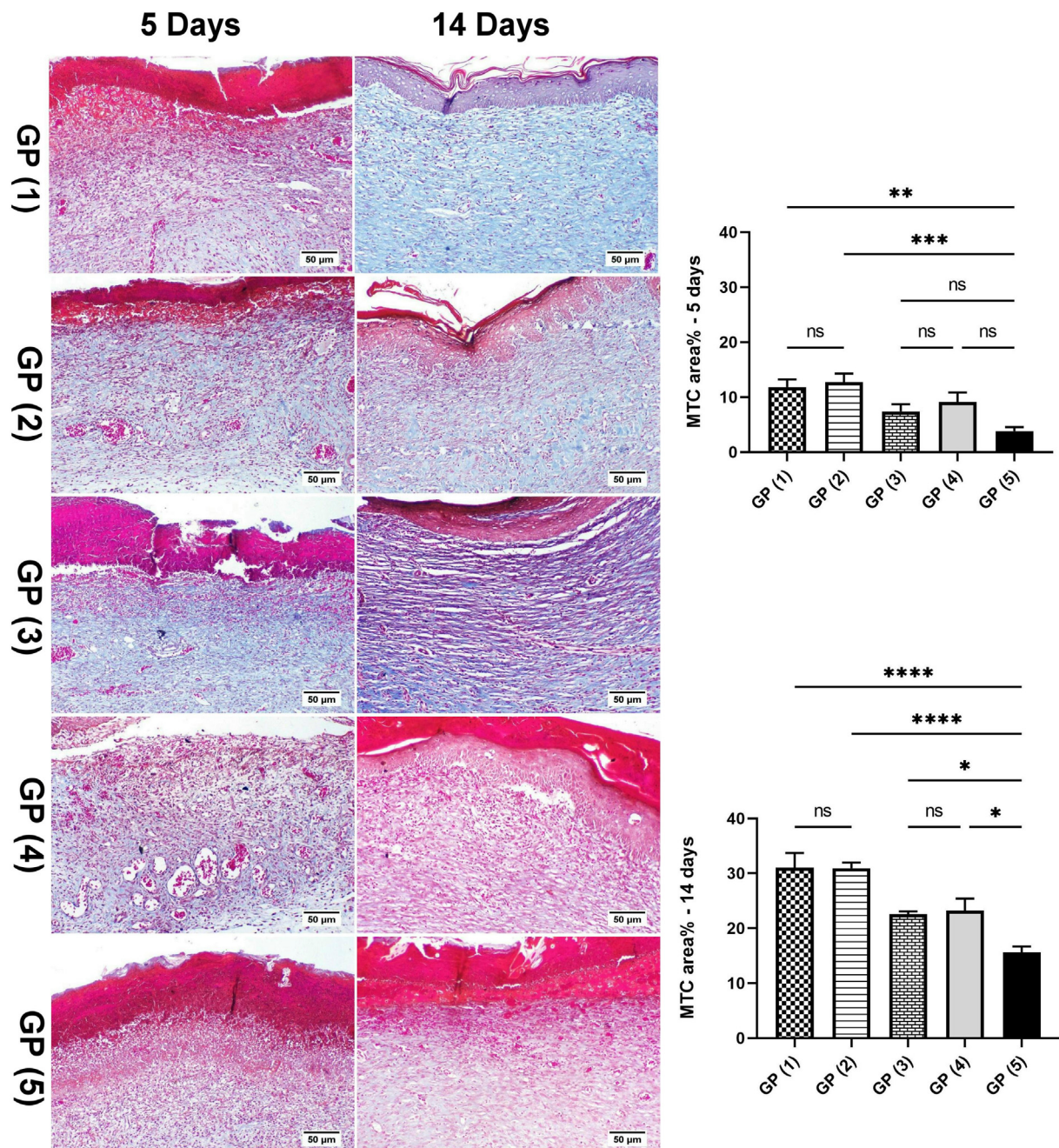

Fig. 11. Masson's trichrome staining of skin sections derived from different groups on days 5 and 14 post-injury. Charts present area % of bluish stained sections in different groups on days 5 and 14. Data Expressed as means ± standard error. A significant difference is considered at p < 0.05.

Fig. 11 showed Masson's trichrome staining of skin sections derived from different groups on day 5 and day 14 post-injury, where the collagen bundles were investigated in the healed wound gaps. At 5 days postsurgical wound induction, a significant enhancement of collagen formation was recorded in GP (1) and GP (2) in comparison with GP (5) that revealed indistinct collagen fibers (bluish stain). Consequently, at 14 days postoperative, collagen bundles showed more extensive deposition and appeared thick and well-organized in GP (1) and GP (2). Fibroblasts produce the continuous synthesis of collagen for numerous weeks during wound repairing (Wang et al., 2017). The collagen formation starts at 3 to 6 days, and density increases until 14 days (Khalaf et al., 2019). Excessive collagen tissue deposition is shared in ECM reconstruction with the additional support of skin growth (Hoveizi et al., 2014). These findings come in agreement with the result obtained with the H&E stain.

These results agree with *in-vitro* and *in-vivo* wound healing studies where groups treated with drug-loaded or un-loaded propolis, and the TTO NE formula showed superiority in re-epithelization and granulation tissue formation anti-inflammation, and angiogenesis in comparison with the other groups. These results indicated that propolis had a significant contribution to the wound healing efficiency of the NE formulae. Propolis shortened the inflammatory phase of wound healing by accelerating debriding activity and reducing the number of inflammatory cells and fibro-vascular areas. Caffeic acid and flavonoids found in propolis reduce the inflammatory response by inhibiting the production of prostaglandins by blocking the lipoxygenase activity leading to immune cells and phagocytes stimulation and make effective anti-inflammatory and analgesic mechanisms like aspirin and with fewer side effects. Also, the bioflavonoids in propolis halt an exodus of inflammatory mediators from mast cells and thereby inhibit the inflammation and allergic reaction (Alqarni et al., 2019). Propolis led to faster wound contraction by increasing collagen type 1 and its major constituent hydroxyproline in the wound. These results agree with the several studies that demonstrated the role of propolis in wound healing using histopathology analysis and found that propolis accelerates the healing process at various phases of tissue repair and reduces the healing time (Abreu et al., 2012; Batista et al., 2012). There was no significant difference among average scores obtained by GP (1) and (2), indicating that the propolis and TTO NE base possess antimicrobial activity comparable to clindamycin-loaded propolis and TTO NE. These results agree with *in-vivo and in-vitro* wound healing assay studies.

4. Conclusions

TTO, propolis, and clindamycin hydrochloride were formulated successfully into NE formulae. The drug un-loaded NE base demonstrated activity comparable to clindamycin-loaded NE. These results pointed to the possibility of reducing the usage of synthetic antibiotics for treating the wound and consequently decreasing the emerging of antibiotic resistance. Also, the results demonstrated the beneficial effect of combining propolis and TTO for efficient wound healing as propolis enhances re-epithelialization, collagen production and has potent anti-inflammatory properties while TTO possesses intense antimicrobial activity. The low viscosity of the NE formula, which was considered a limitation in this study, can be improved by incorporating the NE formula into a suitable gel base. Since these are only preliminary studies, further clinical studies are required to establish the efficacy of these formulations on human skin.

Funding

Declaration of Competing Interest

The authors declare that they have no known competing financial interests or personal relationships that could have appeared to influence the work reported in this paper.

References

Abdellatif, M.M., Khalil, I.A., Khalil, M.A.F., 2017. Sertaconazole nitrate loaded nanovesicular systems for targeting skin fungal infection: In-vitro, ex-vivo and in-vivo evaluation. Int. J. Pharm. 527 (1-2), 1–11. https://doi.org/10.1016/j.ijpharm.2017.05.029.

Abdelrazeg, S., Hussin, H., Salih, M., Shaharuddin, B., 2020. Propolis Composition and Applications in Medicine and Health. Int. Med. J. 25, 1505–1542.

Abreu, A.M., Oliveira, D.W.D., Marinho, S.A., Lima, N.L., de Miranda, J.L., Verli, F.D., 2012. Effect of Topical Application of Different Substances on Fibroplasia in Cutaneous Surgical Wounds. ISRN Dermatol. 2012, 1–5. https://doi.org/10.5402/2012/282973.

Adwan, G.M., Abu-shanab, B.A., Adwan, K.M., 2009. In vitro activity of certain drugs in combination with plant extracts against Staphylococcus aureus infections. African J. Biotechnol. 8, 4239–4241. https://doi.org/10.4314/ajb.v8i17.62364.

Akhtar, J., Siddiqui, H.H., Fareed, S., Badruddeen, Khalid, M., Aqil, M., 2016. Nanoemulsion: for improved oral delivery of repaglinide. Drug Deliv. 23 (6), 2026–2034. https://doi.org/10.3109/10717544.2015.1077290.

Alqarni, A.M., Niwasabutra, K., Sahlan, M., Fearnley, H., Fearnley, J., Ferro, V.A., Watson, D.G., 2019. Propolis exerts an anti-inflammatory effect on pmadifferentiated the-1 cells via inhibition of purine nucleoside phosphorylase. Metabolites 9, 75. https://doi.org/10.3390/metabo9040075.

Barakh Ali, S.F., Dharani, S., Afrooz, H., Khan, M.A., Mohamed, E.M., Kohli, K., Rahman, Z., 2019. Application of salt engineering to reduce/mask bitter taste of clindamycin. Drug Dev. Ind. Pharm. 45 (12), 1871–1878. https://doi.org/10.1080/03639045.2019.1672715.

Batista, L.L.V., Campesatto, E.A., De Assis, M.L.B., Barbosa, A.P.F., Grillo, L.A.M., Dornelas, C.B., 2012. Comparative study of topical green and red propolis in the repair of wounds induced in rats. Rev. Col. Bras. Cir 39, 515–520. https://doi.org/10.1590/S0100-69912012000600012.

Battisti, M.A., Caon, T., Machado de Campos, A., 2021. A short review on the antimicrobial micro- and nanoparticles loaded with Melaleuca alternifolia essential oil. J. Drug Deliv. Sci. Technol. 63, 102283. https://doi.org/10.1016/j.jddst.2020.102283.

Berretta, A.A., Nascimento, A.P., Bueno, P.C.P., Leite Vaz, M.M. de O.L., Marchetti, J. M., 2012. Propolis standardized extract (EPP-AF ®), an innovative chemically and biologically reproducible pharmaceutical compound for treating wounds. Int. J. Biol. Sci. 8, 512–521. https://doi.org/10.7150/ijbs.3641.

Cheesman, M.J., Ilanko, A., Blonk, B., Cock, I.E., 2017. Developing new antimicrobial therapies: Are synergistic combinations of plant extracts/compounds with conventional antibiotics the solution? Pharmacogn. Rev. 11, 57–72. https://doi.org/10.4103/phrev.phrev_21_17.

Chin, K.B., Cordell, B., 2013. The effect of tea tree oil (melaleuca alternifolia) on wound healing using a dressing model. J. Altern. Complement. Med. 19 (12), 942–945. https://doi.org/10.1089/acm.2012.0787.

Dzobo, K., Turnley, T., Wishart, A., Rowe, A., Kallmeyer, K., van Vollenstee, F.A., Thomford, N.E., Dandara, C., Chopera, D., Pepper, M.S., Iqbal Parker, M., 2016. Fibroblast-derived extracellular matrix induces chondrogenic differentiation in human adipose-derived mesenchymal stromal/stem cells in vitro. Int. J. Mol. Sci. 17, 1259. https://doi.org/10.3390/ijms17081259.

Flores, F.C., de Lima, J.A., Ribeiro, R.F., Alves, S.H., Rolim, C.M.B., Beck, R.C.R., da Silva, C.B., 2013. Antifungal Activity of Nanocapsule Suspensions Containing Tea Tree Oil on the Growth of Trichophyton rubrum. Mycopathologia 175, 281–286. https://doi.org/10.1007/s11046-013-9622-7.

Gal, A.F., Stan, L., Tăbăran, F., Rugină, D., Cătoi, A.F., Andrei, S., 2020. Chemopreventive Effects of Propolis in the MNU-Induced Rat Mammary Tumor Model. Oxid. Med. Cell. Longev. 2020. https://doi.org/10.1155/2020/4014838.

Gavanji, S., Larki, B., 2017. Comparative effect of propolis of honey bee and some herbal extracts on Candida albicans. Chin. J. Integr. Med. 23 (3), 201–207. https://doi.org/10.1007/s11655-015-2074-9.

Ghavidel, F., Javadi, A., Anarjan, N., Jafarizadeh-Malmiri, H., 2021. New approach in process intensification based on subcritical water, as green solvent, in propolis oil in water nanoemulsion preparation. Green Process. Synth, 10, 208–218. https://doi.org/10.1515/gps-2021-0022.

Gheib, N., Farzam, A., Habibian, Z., Samiee-Rad, F., 2020. The Effect of Oral Consumption of Propolis Alone and in Combination With Silver Nanoparticles on Wound Healing in Male Wistar Rats. Wound Manag. Prev. 66, 38–46. https://doi.org/10.25270/wmp.2020.4.3846.

Hasan, N., Cao, J., Lee, J., Hlaing, S.P., Oshi, M.A., Naeem, M., Ki, M.H., Lee, B.L., Jung, Y., Yoo, J.W., 2019. Bacteria-targeted clindamycin loaded polymeric nanoparticles: Effect of surface charge on nanoparticle adhesion to MRSA, antibacterial activity, and wound healing. Pharmaceutics 11, 236. https://doi.org/10.3390/pharmaceutics11050236.

Homeyer, D.C., Sanchez, C.J., Mende, K., Beckius, M.L., Murray, C.K., Wenke, J.C., Akers, K.S., 2015. In vitro activity of Melaleuca alternifolia (tea tree) oil on

filamentous fungi and toxicity to human cells. Med. Mycol. 53, 285–294. https://doi.org/10.1093/mmy/myu072.

Hosseini, S.V., Niknahad, H., Fakhar, N., Rezaianzad, A., Mehrabani, D., 2011. The healing effect of mixture of honey, putty, vitriol and olive oil in Pseudomonas aeroginosa infected burns in experimental rat model. Asian J. Anim. Vet. Adv. 6 (6), 572–579. https://doi.org/10.3923/ajava.2011.572.579.

Hoveizi, E., Nabiuni, M., Parivar, K., Rajabi-Zeleti, S., Tavakol, S., 2014. Functionalisation and surface modification of electrospun polylactic acid scaffold for tissue engineering. Cell Biol. Int. 38 (1), 41–49. https://doi.org/10.1002/cbin.10178.

Khalaf, A.A., Hassanen, E.I., Zaki, A.R., Tohamy, A.F., Ibrahim, M.A., 2019. Histopathological, immunohistochemical, and molecular studies for determination of wound age and vitality in rats. Int. Wound J. 16 (6), 1416–1425. https://doi.org/10.1111/iwj.v16.610.1111/iwj.13206.

Li, M., Zhu, L., Liu, B., Du, L., Jia, X., Han, L., Jin, Y., 2016. Tea tree oil nanoemulsions for inhalation therapies of bacterial and fungal pneumonia. Colloids Surfaces B Biointerfaces 141, 408–416. https://doi.org/10.1016/j.colsurfb.2016.02.017.

Lin, H.W., Xie, Q.C., Huang, X., Ban, J.F., Wang, B., Wei, X., Chen, Y.Z., Lu, Z.F., 2018. Increased skin permeation efficiency of imperatorin via charged ultradeformable lipid vesicles for transdermal delivery. Int. J. Nanomedicine 13, 831–842. https://doi.org/10.2147/IJN.S150086.

Main, K.A., Mikelis, C.M., Doçi, C.L., 2020. In vitro wound healing assays to investigate epidermal migration. In: Methods in Molecular Biology. Springer, pp. 147–154. https://doi.org/10.1007/7651_2019_235.

Mikulášová, M., Chovanová, R., Vaverková, Š., 2016. Synergism between antibiotics and plant extracts or essential oils with efflux pump inhibitory activity in coping with multidrug-resistant staphylococci. Phytochem. Rev. 15 (4), 651–662. https://doi.org/10.1007/s11101-016-9458-0.

Mohamed, A.S., Hosney, M., Bassiony, H., Hassanein, S.S., Soliman, A.M., Fahmy, S.R, Gaafar, K., 2020. Sodium pentobarbital dosages for exsanguination affect biochemical, molecular and histological measurements in rats. Scientific Reports 10 (1), 1–13. https://doi.org/10.1038/s41598-019-57252-7.

Muta, T., Parikh, A., Kathawala, K., Haidari, H., Song, Y., Thomas, J., Garg, S., 2020. Quality-by-design approach for the development of nano-sized tea tree oil formulation-impregnated biocompatible gel with antimicrobial properties. Pharmaceutics 12, 1–16. https://doi.org/10.3390/pharmaceutics12111091.

Najafi-Taher, R., Ghaemi, B., Amani, A., 2018. Delivery of adapalene using a novel topical gel based on tea tree oil nanoemulsion: Permeation, antibacterial and safety assessments. Eur. J. Pharm. Sci. 120, 142–151. https://doi.org/10.1016/j.ejps.2018.04.029.

Oh, D.H., Balakrishnan, P., Oh, Y.-K., Kim, D.-D., Yong, C.S., Choi, H.-G., 2011. Effect of process parameters on nanoemulsion droplet size and distribution in SPG membrane emulsification. Int. J. Pharm. 404 (1-2), 191–197. https://doi.org/10.1016/j.ijpharm.2010.10.045.

Olczyk, P., Wisowski, G., Komosinska-Vassev, K., Stojko, J., Klimek, K., Olczyk, M., Kozma, E.M., 2013. Propolis modifies collagen types i and III accumulation in the matrix of burnt tissue. Evidence-based Complement. Altern. Med. 2013, 1–10. https://doi.org/10.1155/2013/423809.

Oliveira, R.N., Mancini, M.C., de Oliveira, F.C.S., Passos, T.M., Quilty, B., Thiré, R.M. da S.M., McGuinness, G.B., 2016. FTIR analysis and quantification of phenols and flavonoids of five commercially available plants extracts used in wound healing. Matéria (Rio Janeiro) 21, 767–779. https://doi.org/10.1590/s1517-707620160003.0072.

Oryan, A., Alemzadeh, E., Moshiri, A., 2018. Potential role of propolis in wound healing: Biological properties and therapeutic activities. Biomed. Pharmacother. 98, 469–483. https://doi.org/10.1016/j.biopha.2017.12.069.

Paknejadi, M., Bayat, M., Salimi, M., Razavilar, V., 2018. Concentration-and time-dependent cytotoxicity of silver nanoparticles on normal human skin fibroblast cell line. Iran. Red Crescent Med. J. 20. https://doi.org/10.5812/ircmj.79183.

Papadimitriou, M., Hatzidaki, E., Papasotiriou, I., 2019. Linearity Comparison of Three Colorimetric Cytotoxicity Assays. J. Cancer Ther. 10 (07), 580–590. https://doi.org/10.4236/jct.2019.107047.

Pazyar, N., Yaghoobi, R., Bagherani, N., Kazerouni, A., 2013. A review of applications of tea tree oil in dermatology. Int. J. Dermatol. 52, 784–790. https://doi.org/10.1111/j.1365-4632.2012.05654.x.

Pereira, R.F., Bártolo, P.J., 2016. Traditional Therapies for Skin Wound Healing. Adv. Wound Care 5 (5), 208–229. https://doi.org/10.1089/wound.2013.0506.

Pessolato, A.G.T., Martins, D.D.S., Ambrósio, C.E., Mançanares, C.A.F., de Carvalho, A. F., 2011. Propolis and amnion reepithelialise second-degree burns in rats. Burns 37 (7), 1192–1201. https://doi.org/10.1016/j.burns.2011.05.016.

Rachmawati, H., Budiputra, D.K., Mauludin, R., 2015. Curcumin nanoemulsion for transdermal application: Formulation and evaluation. Drug Dev. Ind. Pharm. 41 (4), 560–566. https://doi.org/10.3109/03639045.2014.884127.

Ramage, G., Milligan, S., Lappin, D.F., Sherry, L., Sweeney, P., Williams, C., Bagg, J., Culshaw, S., 2012. Antifungal, cytotoxic, and immunomodulatory properties of tea tree oil and its derivative components: Potential role in management of oral candidosis in cancer patients. Front. Microbiol. 3, 220. https://doi.org/10.3389/fmicb.2012.00220.

Salim, N., Ahmad, N., Musa, S.H., Hashim, R., Tadros, T.F., Basri, M., 2016. Nanoemulsion as a topical delivery system of antipsriatic drugs. RSC Adv. 6 (8), 6234–6250. https://doi.org/10.1039/C5RA14946K.

Sari, T.P., Mann, B., Kumar, R., Singh, R.R.B., Sharma, R., Bhardwaj, M., Athira, S., 2015. Preparation and characterization of nanoemulsion encapsulating curcumin. Food Hydrocoll. 43, 540–546. https://doi.org/10.1016/j.foodhyd.2014.07.011.

Shehata, M.G., Ahmad, F.T., Badr, A.N., Masry, S.H., El-Sohaimy, S.A., 2020. Chemical analysis, antioxidant, cytotoxic and antimicrobial properties of propolis from different geographic regions. Ann. Agric. Sci. 65 (2), 209–217. https://doi.org/10.1016/j.aoas.2020.12.001.

Singh, Y., Meher, J.G., Raval, K., Khan, F.A., Chaurasia, M., Jain, N.K., Chourasia, M.K., 2017. Nanoemulsion: Concepts, development and applications in drug delivery. J. Control. Release 252, 28–49. https://doi.org/10.1016/j.jconrel.2017.03.008.

Sinha, P., Srivastava, S., Mishra, N., Singh, D.K., Luqman, S., Chanda, D., Yadav, N.P., 2016. Development, optimization, and characterization of a novel tea tree oil nanogel using response surface methodology. Drug Dev. Ind. Pharm. 42 (9), 1434–1445. https://doi.org/10.3109/03639045.2016.1141931.

Tas, C., Ozkan, Y., Okyar, A., Savaser, A., 2007. In vitro and ex vivo permeation studies of etodolac from hydrophilic gels and effect of terpenes as enhancers. Drug Deliv. 14 (7), 453–459. https://doi.org/10.1080/10717540701603746.

Thomas, L., Zakir, F., Mirza, M.A., Anwer, M.K., Ahmad, F.J., Iqbal, Z., 2017. Development of Curcumin loaded chitosan polymer based nanoemulsion gel: In vitro, ex vivo evaluation and in vivo wound healing studies. Int. J. Biol. Macromol. 101, 569–579. https://doi.org/10.1016/j.ijbiomac.2017.03.066.

Wagh, V.D., 2013. Propolis: A wonder bees product and its pharmacological potentials. Adv. Pharmacol. Sci. 2013, 1–11. https://doi.org/10.1155/2013/308249.

Wang, J., Hao, S., Luo, T., Cheng, Z., Li, W., Gao, F., Guo, T., Gong, Y., Wang, B., 2017. Feather keratin hydrogel for wound repair: Preparation, healing effect and biocompatibility evaluation. Colloids Surfaces B Biointerfaces 149, 341–350. https://doi.org/10.1016/j.colsurfb.2016.10.038.

Wulansari, A., Jufri, M., Budianti, A., 2017. Studies on the formulation, physical stability, and in vitro antibacterial activity of tea tree oil (Melaleuca alternifolia) nanoemulsion gel. Int. J. Appl. Pharm. 9, 135–139. https://doi.org/10.22159/ijap.2017.v9s1.73_80.